Supporting Information

Effect of carbon and nitrogen double vacancies on the improved photocatalytic hydrogen evolution over porous carbon nitride nanosheets

*Huihui Li [*1], Fuchun Ning[1], Xiaofei Chen, Anye Shi*

National & Local Joint Engineering Laboratory for Optical Conversion Materials and Technology, Key Laboratory of Special Function Materials and Structure Design, Ministry of Education, Lanzhou University, 222 South Tianshui Road, Lanzhou 730000, China

[*]Corresponding author: lihh@lzu.edu.cn

[1]These authors are co-first authors.

Contents Page

Generally, the porous structure can be obtained by using silica nanoparticles as hard templates [s1-s3]. However, the hard template removal process usually brings the hazardous and toxic issues. As an alternative, the soft template method is a more facile and simple way to fabricate the porous structure. Hou et al. reported that a worm-like porous carbon nitride synthesized by using Pluronic P123 as soft-template [s4]. Li et al. could obtain hierarchically porous carbon nitride by using polyurethane as single template [s5]. One-step pyrolysis treatment of dicyandiamide and ammonium persulphate can also be applied for the formation of porous carbon nitride [s6]. In addition, the soft template method can also be performed to prepare ultrathin carbon nitride, e.g. we can obtain a single atomic layered carbon nitride nanosheets in large scale by using polyacrylamide (PAM) as the template with melamine precursor [s7].

First, XRD characterization was carried out to investigate the effects of PVP template content and heating period on the crystal structure of carbon nitride samples. As presented in Fig. S1a-b, all the XRD patterns show two characteristic peaks located at about 12.6° and 27.4°, corresponding to the 100 and 002 crystal planes, respectively. Then, the morphology of samples was observed through TEM images (Fig. S2a-b). It is clear that the size and number of holes increase with increasing the concentration of PVP precursor and extending the heating time. The absorption in visible light region also increase with the increase content of PVP (Fig. S3a), while the extension of heating time results in a slight blue-shift of DRS curve (Fig. S3b). Moreover, as shown in Fig. S4a-b, PL spectra suggest that the increase content of PVP and extended heating time benefit for the separation of photogenerated electron-hole pairs. More PVP precursor and longer heating time show positive effects on the degradation of RhB dyes solution over carbon nitride photocatalyst (Fig. S5a-b). Therefore, the porous carbon nitride nanosheets is prepared by using 10 g of melamine and 500 mL of PVP (100 g L-1) as precursors and heating the mixture at 550 ºC for 8

h. Then, the following investigation was carried out based on the comparison between the porous carbon nitride with the optimal preparation (CN-PVP) and pristine one (BCN).

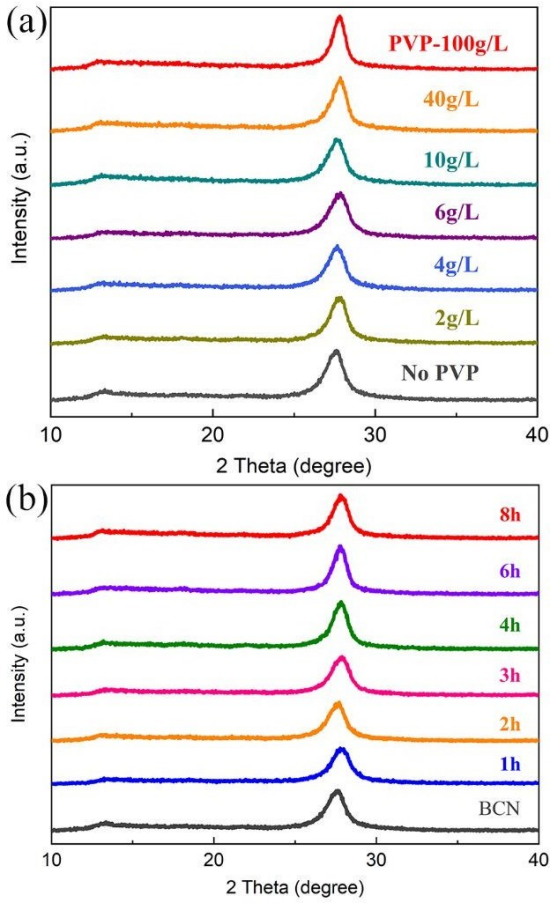

Fig S1. XRD patterns of BCN and all the CN-PVP samples with (a) different content of PVP precursors after heating at 550 °C for 4 h or (b) the same 2 g/L of PVP but different keeping time at 550 °C.

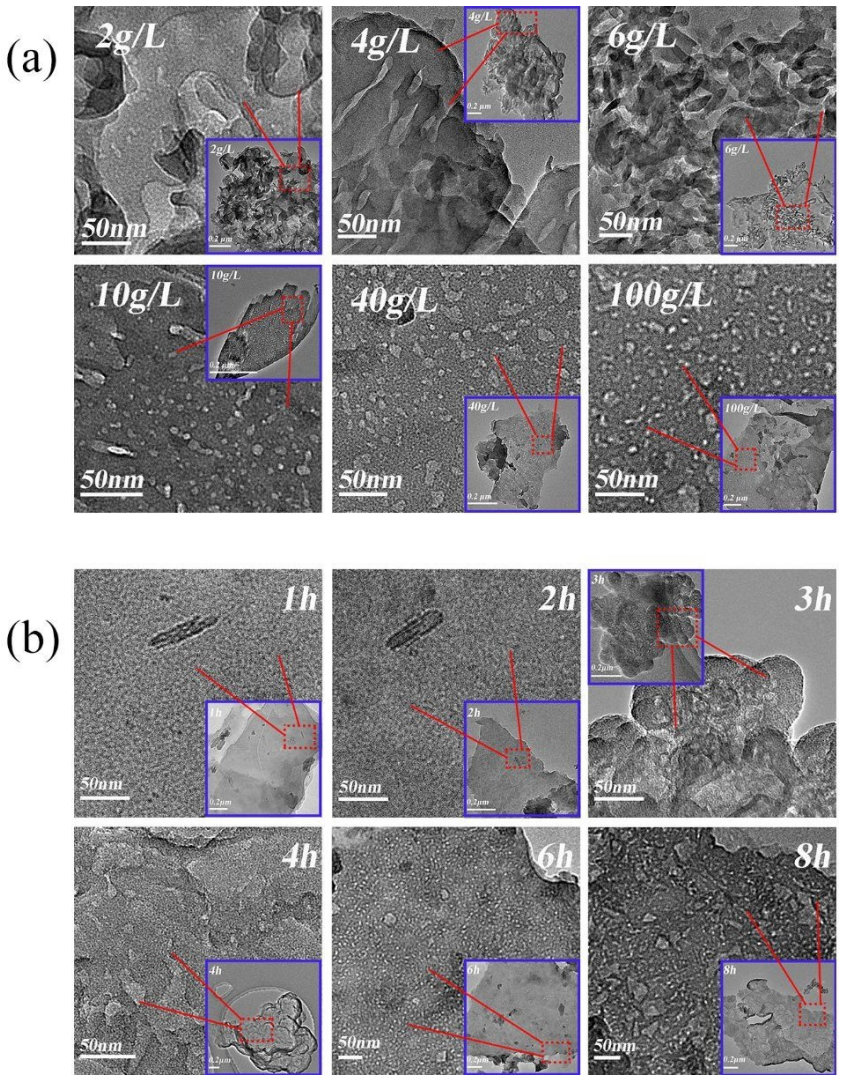

Fig S2. TEM images of carbon nitride samples with (a) different content of PVP precursors after heating at 550 °C for 4 h or (b) the same 2 g/L of PVP but different keeping time at 550 °C.

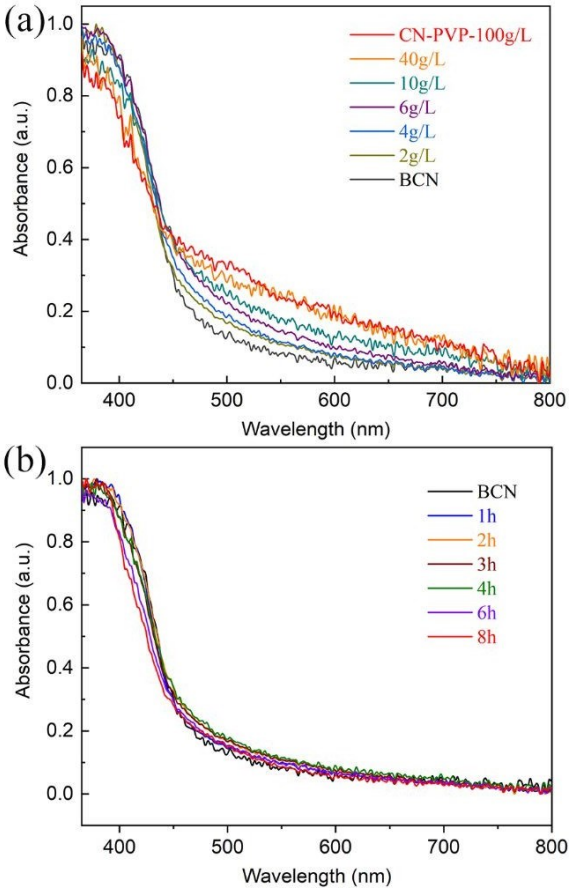

Fig S3. UV-vis absorption spectra of carbon nitride samples with (a) different content of PVP precursors after heating at 550 °C for 4 h or (b) the same 2 g/L of PVP but different keeping time at 550 °C.

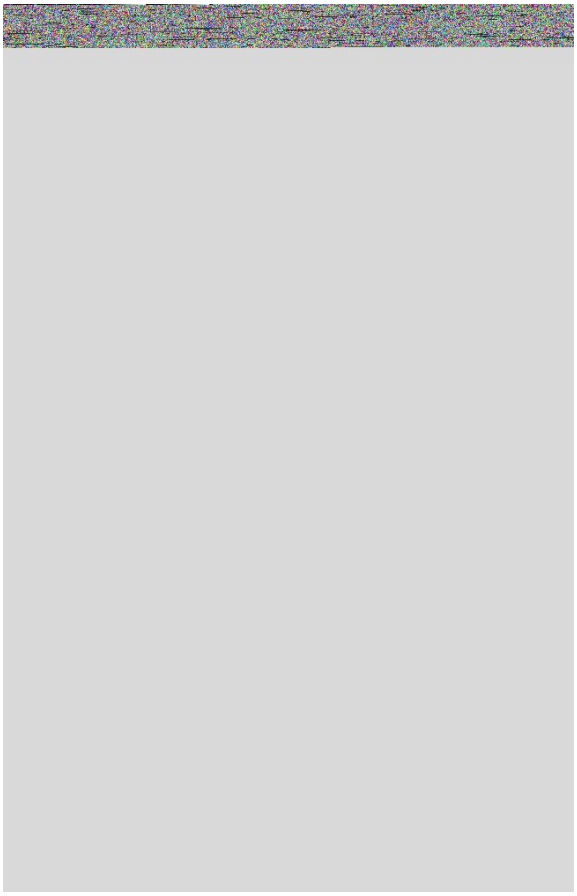

Fig S4. PL spectra of carbon nitride samples with (a) different content of PVP precursors after heating at 550 °C for 4 h or (b) the same 2 g/L of PVP but different keeping time at 550 °C.

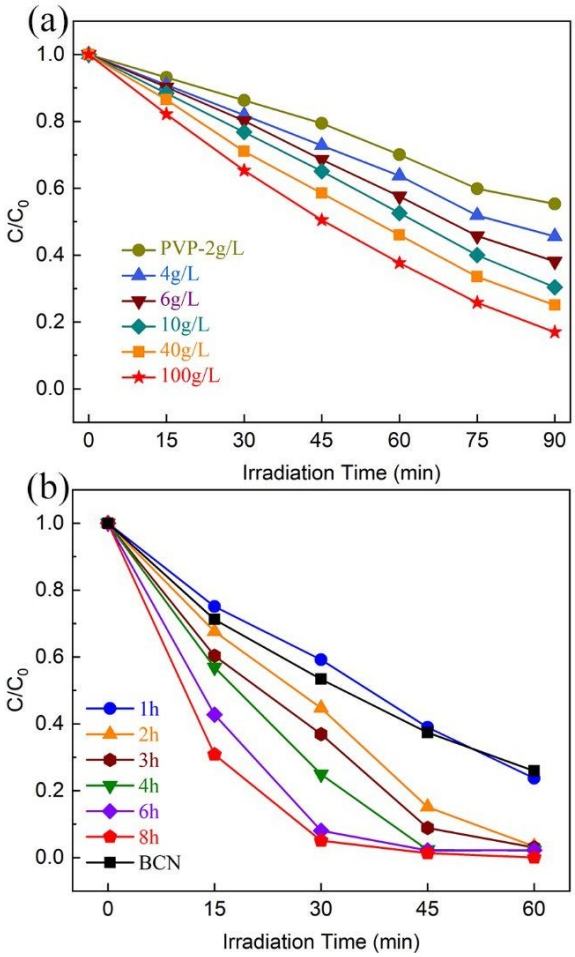

Fig S5. Photocatalytic degradation of RhB dyes solution over carbon nitride with (a) different content of PVP precursors after heating at 550 °C for 4 h or (b) the same 2 g/L of PVP but different keeping time at 550 °C. Light source: white LED lamp; photocatalyst amount: (a) 5 mg and (b) 30 mg; RhB dyes solution: 20 mg/L, 50 mL.

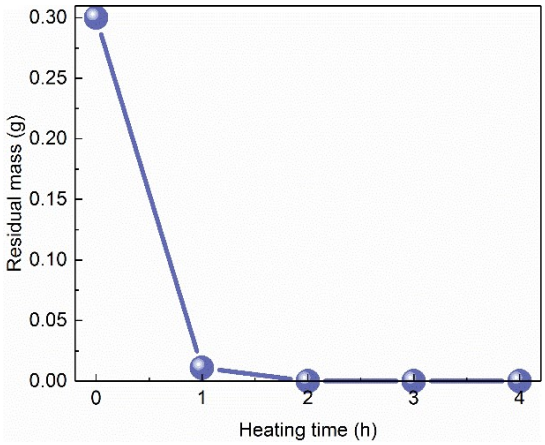

Fig S6. Residual amount of PVP after heating at 450 °C for different time.

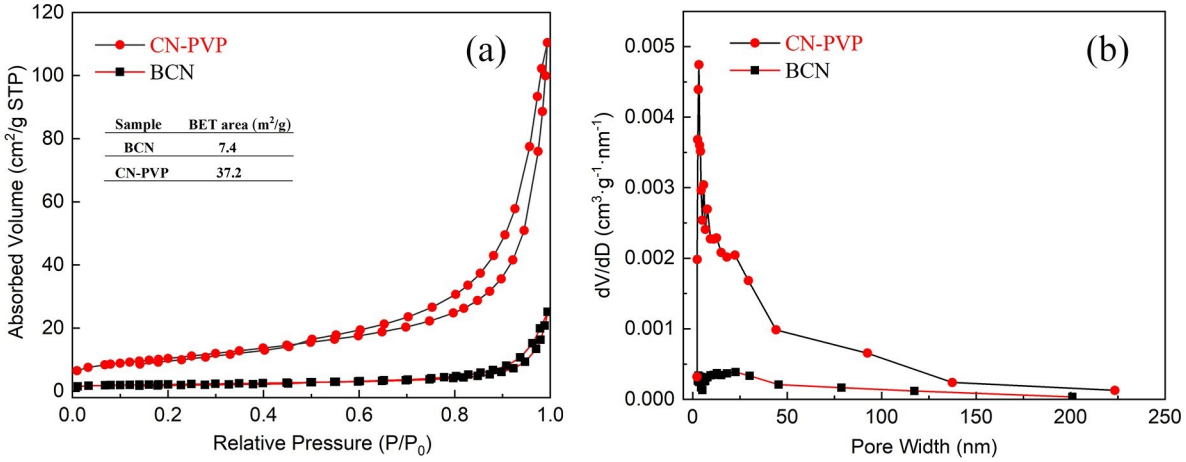

Fig S7. (a) N_2 absorption-desorption isotherms and (b) the corresponding pore diameter distributions of BCN and CN-PVP.

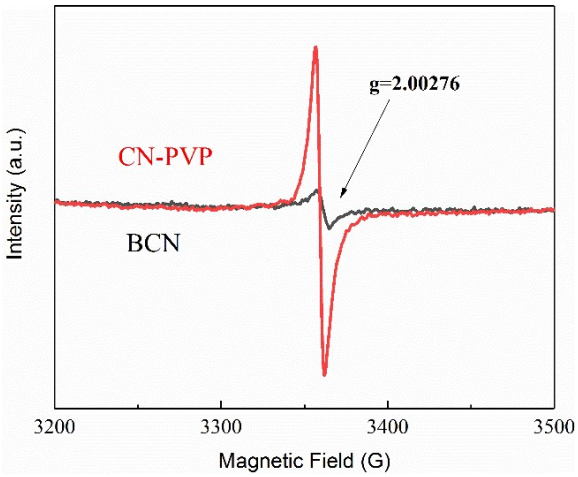

Fig S8. EPR spectra of BCN and CN-PVP.

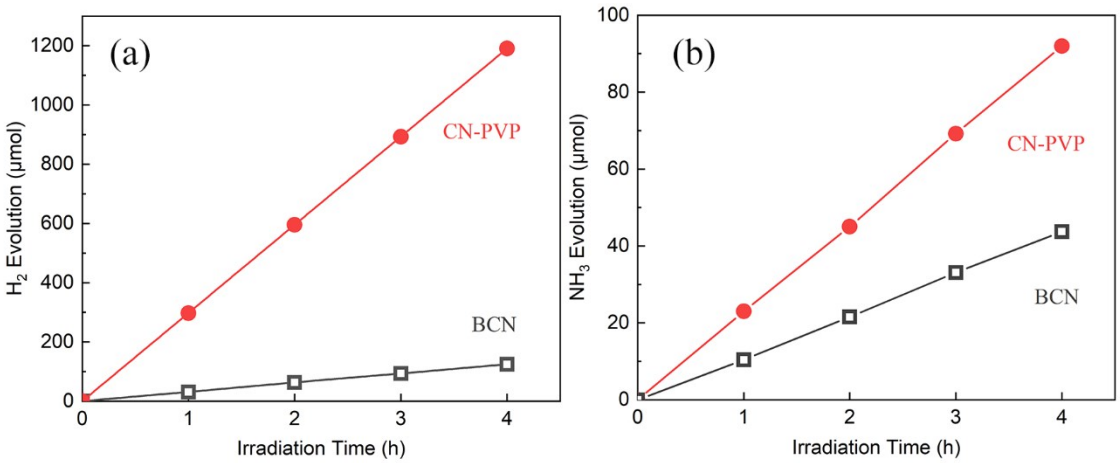

Fig S9. Time courses of (a) H_2 and (b) NH_3 evolution over different carbon nitride samples under white LED lamp irradiation.

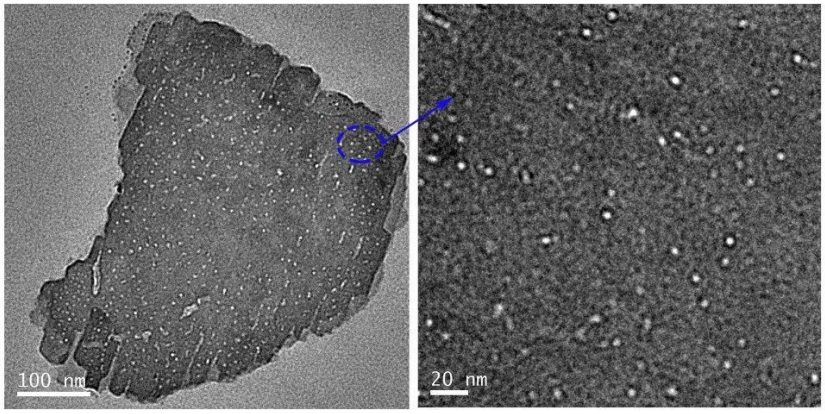

Fig S10. TEM images of CN-PVP after cycling experiment.

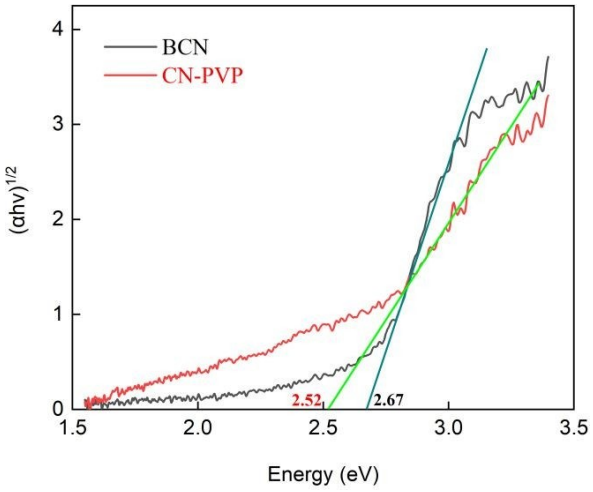

Fig S11. Plots of $(\alpha hv)^{0.5}$ versus the energy of exciting light.

Table S1 Combustion elemental analysis results of BCN and CN-PVP.

Sample[a]	Mass content (%)			
	C	N	H	C/N
1H	34.1	59.3	1.6	0.574
2H	34.2	59.0	1.6	0.580
BCN	34.9	59.8	1.6	0.584
3H	34.1	58.2	1.6	0.586
4H	34.4	58.5	1.6	0.588
4G	34.6	58.7	1.6	0.590
6G	34.5	58.3	1.7	0.591
6H	34.2	57.8	1.7	0.592
10G	34.1	57.4	1.9	0.594
8H	34.8	58.3	2.0	0.596
40G	34.4	57.7	2.1	0.597
100G	34.6	57.4	2.2	0.603
CN-PVP	34.7	57.4	2.2	0.606

[a.] xH: samples were synthesized under different holding time but adding the same PVP (2 g L^{-1}), yG: samples were synthesized under the same 4 h holding time but using different PVP precursors (y g L^{-1}), all the samples were heated at 823 K.

Table S2. Photocatalytic H_2 evolution of typical carbon nitride porous nanosheets.

Ref.	Photocatalyst (mg)	Water (mL)	TEOA (vol.%)	Pt (wt.%)	H_2 evolution rate (μmol h^{-1})	AQY (%) at 420 nm
This work	100	100	10	1	297.6	12.7
s8	50	280	10	3	195.8	6.1
s9	100	300	10	3	132.3	7.45
s10	20	120	10	3	60.2	7.8
s11	10	25	10	3	82.9	--
s12	100	300	10	3	107.8	--
s13	20	50	10	3	57.2	--
s14	50	120	10	3	98.4	10.7
s15	10	100	10	3	20.9	1.46
s16	50	80	15	3	200	14.65
s17	15	20	10	-	90	--
s18	30	80	10	1	11.6	8.54
s19	50	100	10	5	81.7	8.29
s20	50	100	10	1	64.3	12.06
s21	20	100	20	1	159.8	9.8
s22	50	100	20	3	180.63	8.6
s23	50	--	20	1	79.8	3.56
s24	50	100	10	3	189.3	--
s25	50	200	10	5	44.6	6.84
s26	50	50	20	3	155	28
s27	10	80	10	3	12.71	--

Table S3. Summary of the relationship between photocatalytic activity and the ratio of C/N over all carbon nitride samples.

Sample[a]	C/N[b]	H_2 evolution rate[c] (μmol h^{-1})	Dyes degradation[d] (1-C/C_0, %)			
			MB	RhB	MO	Phenol
1H	0.574	17.2	30.3	40.8	6.4	0.6
2H	0.580	27.3	30.3	55.3	10.9	1.0
BCN	0.584	31.2	30.8	58.1	11.0	4.2
3H	0.586	35.1	31.6	63.1	12.2	4.5
4H	0.588	43.9	30.5	75.1	13.9	8.1
4G	0.590	57.5	35.7	86.7	15.5	10.7
6G	0.591	69.9	37.5	89.5	18.2	14.0
6H	0.592	72.3	32.1	89.3	15.8	13.1
10G	0.594	100.6	42.9	87.9	19.9	23.3
8H	0.596	93.5	44.0	88.7	21.3	25.7
40G	0.597	128.7	44.8	92.0	18.2	26.8
100G	0.603	140.0	46.0	93.4	22.9	29.2
CN-PVP	0.606	297.6	76.1	95.0	26.3	36.9

[a.] xH: samples were synthesized under different holding time but adding the same PVP (2 g L^{-1}), yG: samples were synthesized under the same 4 h holding time but using different PVP precursors (y g L^{-1}), all the samples were heated at 823 K.

[b.] The weight ratio of carbon to nitrogen is monitored by combustion elemental analysis.

[c.] Photocatalytic water splitting reaction condition: 100 mg of Pt (1.0 wt.%)-sample, 100 mL of TEOA (10 vol.%) aqueous solution, an outer irradiation quartz reactor, white LED lamp (100 mW cm^{-2}, 365~940 nm).

[d.] Dyes degradation reaction condition: 30 mg sample, 50 ml of dyes aqueous solution (10 mg L^{-1}).

Table S4. Fractions of C 1s XPS spectra.

Sample	Peak location (eV)		
	288.1(N-C=N)	286.2(C-NH_x)	284.6(C-C)
BCN	0.7	0	0.3
CN-PVP	0.6	0.1	0.3

Table S5. Fractions of N 1s XPS spectra.

Sample	Peak location (eV)			
	398.6(C-N=C)	400.1(N-$(C)_3$)	401.2(C-NH_x)	404.3
BCN	0.6	0.2	0.1	0.1
CN-PVP	0.6	0.1	0.2	0.1

Reference

[s1] X. Wang, K. Maeda, X. Chen, K. Takanabe, K. Domen, Y. Hou, X. Fu and M. Antonietti, Polymer Semiconductors for Artificial Photosynthesis: Hydrogen Evolution by Mesoporous Graphitic Carbon Nitride with Visible Light, *J. Am. Chem. Soc.*, 2009, **131**, 1680-1681.

[s2] M. Antonietti and M. Groenewolt, Synthesis of g-C_3N_4 Nanoparticles in Mesoporous Silica Host Matrices, *Adv. Mater.*, 2005, **17**, 1789.

[s3] F. Goettmann, A. Fischer, M. Antonietti and A. Thomas, A. Chemical Synthesis of Mesoporous Carbon Nitrides Using Hard Templates and Their Use as a Metal-Free Catalyst for Friedel-Crafts Reaction of Benzene, *Angew. Chem., Int. Ed.*, 2006, **45**, 4467.

[s4] H. Yan, Soft-templating synthesis of mesoporous graphitic carbon nitride with enhanced photocatalytic H_2 evolution under visible light, *Chem. Commun.*, 2012, **48**, 3430.

[s5] Y. Li, Z. Ruan, Y. He, J. Li, K. Li, Y. Jiang, X. Xu, Y. Yuan and K. Lin, In situfabrication of hierarchically porous g-C_3N_4 and understanding on its enhanced photocatalytic activity based on energy absorption, *Appl. Catal. B*, 2018, **236**, 64-75.

[s6] Y. Jiang, Z. Sun, C. Tang, Y. Zhou, L. Zeng and L. Huang, Enhancement of photocatalytic hydrogen evolution activity of porous oxygen doped g-C_3N_4 with nitrogen defects induced by changing electron transition, *Appl. Catal. B*, 2019, **240**, 30-38.

[s7] A. Shi, H. Li, S. Yin, B. Liu, J. Zhang and Y. Wang, Effect of conjugation degree and delocalized -system on the photocatalytic activity of single layer g-C_3N_4, *Appl. Catal. B*, 2017, **218**, 137-146.

[s8] L. Shi, K. Chang, H. Zhang, X. Hai, L. Yang, T. Wang and J. Ye, Drastic Enhancement of Photocatalytic Activities over Phosphoric Acid Protonated Porous g-C_3N_4 Nanosheets under Visible Light, *Small,* 2016, **12**, 4431-4439.

[s9] W. Xing, G. Chen, C. Li, Z. Han, Y. Hu and Q. Meng, Doping effect of non-metal group in porous ultrathin g-C_3N_4 nanosheets towards synergistically improved photocatalytic hydrogen evolution, *Nanoscale*, 2018, **10**, 5239-5245.

[s10] Z. Huang, J. Song, L. Pan, Z. Wang, X. Zhang, J. Zou, W. Mi, X. Zhang and L. Wang, Carbon nitride with simultaneous porous network and O-doping for efficient solar-energy-driven hydrogen evolution, *Nano Energy*, 2012, **12**, 646-656.

[s11] Q. Liang, Z. Li, Z. Huang, F. Kang and Q. Yang, Holey Graphitic Carbon Nitride Nanosheets with Carbon Vacancies for Highly Improved Photocatalytic Hydrogen Production, *Adv. Funct. Mater.*, 2015, **25**, 6885–6892.

[s12] F. He, G. Chen, Y. Zhou, Y. Yu, Y. Zheng and S. Hao, Facile synthesis of mesoporous g-C_3N_4 with highly enhanced photocatalytic H_2 evolution performance, *Chem. Commun.*, 2015, **51**, 16244-16246.

[s13] Y. Li, R. Jin, Y. Xing, J. Li, S. Song, X. Liu, M. Li and R. Jin. Macroscopic Foam-Like Holey Ultrathin g-C_3N_4 Nanosheets for Drastic Improvement of Visible-Light Photocatalytic Activity, *Adv. Energy Mater.*, 2016, **6**, 1601273.

[s14] J. Zhang, S. Gong, N. Mahmood, L. Pan, X. Zhang and J. Zou, Oxygen-doped nanoporous carbon nitride via water-based homogeneous supramolecular assembly for photocatalytic hydrogen evolution, *Appl. Catal. B*, 2018, **221**, 9-16.

[s15] D. Zhang, Y. Guo and Z. Zhao, Porous defect-modified graphitic carbon nitride via a facile one-step approach with significantly enhanced photocatalytic hydrogen evolution under visible light irradiation, *Appl. Catal. B*, 2018, **226**, 1-9.

[s16] J. Yuan, X. Liu, Y. Tang, Y. Zeng, L. Wang, S. Zhang, T. Cai, Y. Liu, S. Liu, Y. Pei and C. Liu, Positioning cyanamide defects in g-C_3N_4: Engineering energy levels and active sites for superior photocatalytic hydrogen evolution, *Appl. Catal. B*, 2018, **237**, 24-31.

[17] J. Bai, C. Yin, H. Xu, G. Chen, Z. Ni, Z. Wang, Y. Li, S. Kang, Z. Zheng and X. Li, Facile urea-assisted precursor pre-treatment to fabricate porous g-C_3N_4 nanosheets for remarkably enhanced visible-light-driven hydrogen evolution, *J. Colloid Interf. Sci.*, 2018, **532**, 280-286.

[s18] Z. Yang, D. Chu, G. Jia, M. Yao and B. Liu, Significantly narrowed bandgap and enhanced charge separation in porous, nitrogen-vacancy red g-C_3N_4 for visible light photocatalytic H_2 production, *Appl. Surf. Sci.*, 2020, **504**, 144407.

[s19] J. Wu, N. Li, H. Fang, X. Li, Y. Zheng and X. Tao, Nitrogen vacancies modified graphitic carbon nitride: Scalable and one-step fabrication with efficient visible-light-driven hydrogen evolution, *Chem. Eng. J.*, 2019, **358**, 20-29.

[s20] P. Song, S. Liang, J. Cui, D. Ren, R. Duan, Q. Yang and S. Sun, Purposefully designing novel hydroxylated and carbonylated melamine towards to the synthesis of targeted porous oxygen-doped g-C_3N_4 nanosheets for highly enhanced photocatalytic hydrogen production, *Catal. Sci. Technol.*, 2019, **9**, 5150-5159.

[s21] Y. Xiao, G. Tian, W. Li, Y. Xie, B. Jiang, C. Tian. D. Zhao and H. Fu, Molecule Self-Assembly Synthesis of Porous Few-Layer Carbon Nitride for Highly Efficient Photoredox Catalysis, *J. Am. Chem. Soc.*, 2019, **141**, 2508-2515.

[s22] H. Che, C. Liu, G. Che, G. Liao, H. Dong, C. Li, N. Song and C. Li, Facile construction of porous intramolecular g-C_3N_4-based donor-acceptor conjugated copolymers as highly efficient photocatalysts for superior H_2 evolution, *Nano Energy*, 2020, **67**, 104273.

[s23] J. Ran, T. Ma, G. Gao, X. Du and S. Qiao, Porous P-doped graphitic carbon nitride nanosheets for synergistically enhanced visible-light photocatalytic H_2 production, *Energy Environ. Sci.*, 2015, **8**, 3708-3717.

[s24] X. She, L. Liu, H. Ji, Z. Mo, Y. Li, L. Huang, D. Du, H. Xu and H. Li, Template-free synthesis of 2D porous ultrathin nonmetal-doped g-C_3N_4 nanosheets with highly efficient photocatalytic H_2 evolution from water under visible light, *Appl. Catal. B*, 2016, **187,** 144-153.

[s25] Y. Zhang, S. Zong, C. Cheng, J. Shi, P. Guo, X. Guan, B. Luo, S. Shen and L. Guo, Rapid high-temperature treatment on graphitic carbon nitride for excellent photocatalytic H_2-evolution performance, *Appl. Catal. B*, 2018, **233**, 80-87.

[s26] D. Ruan, S. Kim, M. Fujitsuka, T. Majima, Defects rich g-C_3N_4 with mesoporous structure for efficient photocatalytic H_2 production under visible light irradiation, *Appl. Catal. B*, 2018, **238**, 638-646.

[s27] X. Wang, L. Wu, Z. Wang, H. Wu, X. Zhou, H. Ma, H. Zhong, Z. Xing, G. Cai, C. Jiang and F. Ren, C/N Vacancy Co-Enhanced Visible-Light-Driven Hydrogen Evolution of g-C_3N_4 Nanosheets Through Controlled He^+ Ion Irradiation, *Sol. RRL*, 2019, **3**, 1800298.